You might find this additional information useful...

This article cites 9 articles, 7 of which you can access free at:
http://jn.physiology.org/cgi/content/full/87/2/1129#BIBL

This article has been cited by 28 other HighWire hosted articles, the first 5 are:

Neuronal network analyses: premises, promises and uncertainties
D. Parker
Phil Trans R Soc B, August 12, 2010; 365 (1551): 2315-2328.
[Abstract] [Full Text] [PDF]

Computational approaches to neuronal network analysis
A. A. Prinz
Phil Trans R Soc B, August 12, 2010; 365 (1551): 2397-2405.
[Abstract] [Full Text] [PDF]

Compensation for Variable Intrinsic Neuronal Excitability by Circuit-Synaptic Interactions
R. Grashow, T. Brookings and E. Marder
J. Neurosci., July 7, 2010; 30 (27): 9145-9156.
[Abstract] [Full Text] [PDF]

Subject-Specific Muscle Synergies in Human Balance Control Are Consistent Across Different Biomechanical Contexts
G. Torres-Oviedo and L. H. Ting
J Neurophysiol, June 1, 2010; 103 (6): 3084-3098.
[Abstract] [Full Text] [PDF]

Model Calcium Sensors for Network Homeostasis: Sensor and Readout Parameter Analysis from a Database of Model Neuronal Networks
C. Gunay and A. A. Prinz
J. Neurosci., February 3, 2010; 30 (5): 1686-1698.
[Abstract] [Full Text] [PDF]

Medline items on this article's topics can be found at http://highwire.stanford.edu/lists/artbytopic.dtl
on the following topics:
Physiology .. Membrane Potential
Physiology .. Action Potential

Updated information and services including high-resolution figures, can be found at:
http://jn.physiology.org/cgi/content/full/87/2/1129

Additional material and information about *Journal of Neurophysiology* can be found at:
http://www.the-aps.org/publications/jn

This information is current as of August 25, 2010 .

Failure of Averaging in the Construction of a Conductance-Based Neuron Model

JORGE GOLOWASCH,[1] MARK S. GOLDMAN,[1,2] L. F. ABBOTT,[1] AND EVE MARDER[1]
[1]*Volen Center for Complex Systems and Department of Biology, Brandeis University, Waltham 02454; and*
[2]*Department of Physics, Harvard University, Cambridge, Massachusetts 02138*

Golowasch, Jorge, Mark S. Goldman, L. F. Abbott, and Eve Marder. Failure of averaging in the construction of a conductance-based neuron model. *J Neurophysiol* 87: 1129–1131, 2002; 10.1152/jn.00412.2001. Parameters for models of biological systems are often obtained by averaging over experimental results from a number of different preparations. To explore the validity of this procedure, we studied the behavior of a conductance-based model neuron with five voltage-dependent conductances. We randomly varied the maximal conductance of each of the active currents in the model and identified sets of maximal conductances that generate bursting neurons that fire a single action potential at the peak of a slow membrane potential depolarization. A model constructed using the means of the maximal conductances of this population is not itself a one-spike burster, but rather fires three action potentials per burst. Averaging fails because the maximal conductances of the population of one-spike bursters lie in a highly concave region of parameter space that does not contain its mean. This demonstrates that averages over multiple samples can fail to characterize a system whose behavior depends on interactions involving a number of highly variable components.

INTRODUCTION

Measurements of neuronal conductances often exhibit a large degree of variability (Gardner 1993; Golowasch et al. 1999; Liu et al. 1998). It is customary to characterize such data using means and variances. For example, mean conductance values are typically used to set the parameters of a model constructed to simulate neuronal activity. If the resulting model fails to capture the behavior of the neuron being modeled, the parameters are normally adjusted within a region characterized by the variances of the measured values. It has been suggested previously that such a program can fail (Beer et al. 1999; Foster et al. 1993; Goldman et al. 2001). Here we present an example that illustrates this problem and suggests when it will occur. We use a population of model neurons as our data and show that a model built with parameters set to averages of the corresponding conductances, or to most of the values within a 1 SD covariance ellipse about the mean, fails to match the behavior of the neurons that were used to generate the data. In this example, averaging fails not as a result of measurement error, but because the distribution of data points is poorly characterized by its mean and variance or even other higher order statistical measures. Specifically, the mean and most of the 1 SD covariance ellipse do not lie within the distribution from which they are computed.

METHODS

Electrophysiology

Experimental methodology follows that described previously (Golowasch et al. 1999). We used two-electrode voltage clamp to measure the peak conductances of three K^+ currents (I_{Kd}, I_{KCa}, and I_A) expressed in isolated inferior cardiac (IC) neurons of the stomatogastric ganglion of the crab *Cancer borealis*. The IC neuron was isolated by adding 10^{-5} M picrotoxin (PTX) and 10^{-7} M tetrodotoxin (TTX) to the bath. Peak conductances were calculated at +20 mV, assuming a potassium reversal potential of −80 mV. Currents were separated as described previously (Golowasch et al. 1999).

Model description

A single compartment conductance-based model was built using standard Hodgkin-Huxley equations to describe five voltage-dependent conductances (Na^+ conductance, *gNa;* delayed-rectifier K^+ conductance, *gKd;* A-type K^+ conductance, *gA;* Ca^{2+}-activated K^+ conductance, *gKCa;* and Ca^{2+} conductance, *gCa*) and a fixed voltage-independent leak current. The kinetics and voltage dependence of these conductances are based on measurements performed on cultured stomatogastric ganglion (STG) neurons (Turrigiano et al. 1995) and are exactly as described in Liu et al. (1998). In our model, we fixed the ratio of the maximal conductances of the fast and slow Ca^{2+} currents (CaT and CaS in Liu et al. 1998) at 1.25. Values reported are for the fast component only. Buffering of Ca^{2+} (used in computing I_{KCa}) follows the model described previously (Liu et al. 1998), but with a buffering time constant of 200 ms.

We chose maximum conductances for the currents randomly from uniform distributions over the ranges (in mS/cm²): $g_{max}Na$, 0–800; $g_{max}Kd$, 0–200; $g_{max}Ca$, 0–5; $g_{max}A$, 0–75; $g_{max}KCa$, 0–300; *gLeak*, fixed at 0.01. These distributions all have SD to mean ratios of $1/\sqrt{3}$, which sets the scale for the variability seen in the model. The model was integrated numerically using a second-order accurate, stable method with adaptive step size.

RESULTS

Each class of identified neurons of the crustacean STG displays a characteristic and stereotyped firing pattern. Nonetheless, voltage-clamp measurements of three K^+ currents
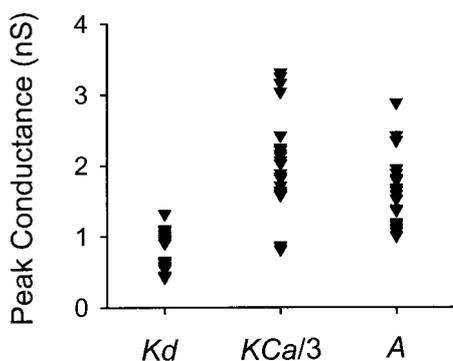
FIG. 1. Variation in the peak conductances of 3 K$^+$ conductances for a neuron of the crab stomatogastric ganglion (STG). Peak conductances measured in the inferior cardiac (IC) neuron of 22 different preparations vary over a factor of 3.1 for *gKd*, 4.0 for *gKCa*, and 2.9 for *gA*. Means and SDs for the 3 conductances are as follows: *gKd* = 0.77 ± 0.27 nS, *gKCa* = 6.05 ± 2.15 nS, *gA* = 1.58 ± 0.50 nS. A subset of these data has been published in different form previously in Golowasch et al. (1999).

show a three- to fourfold variability in peak conductance (Fig. 1). To mimic the variability seen in such conductance data, we built 2,000 model neurons by randomly choosing sets of maximal conductances (Bhalla and Bower 1993; Foster et al. 1993; Goldman et al. 2001) for the 5 voltage-dependent currents of the model (METHODS). We classified the resulting patterns of activity as silent, tonically firing action potentials, or bursting
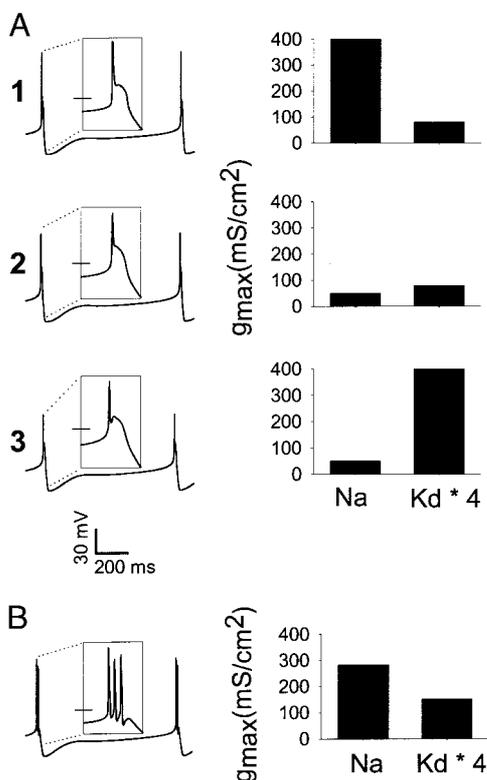

FIG. 2. Failure of averaging in a conductance-based model neuron. *A, left panels*: voltage traces for 3 observed one-spike bursters. Conductance values in mS/cm^2: 1, $g_{max}Na$ = 400, $g_{max}Kd$ = 20.0; 2, $g_{max}Na$ = 50.0, $g_{max}Kd$ = 20.0; 3, $g_{max}Na$ = 50.0, $g_{max}Kd$ = 100; all 3, $g_{max}Ca$ = 4.0, $g_{max}A$ = 5.0, $g_{max}KCa$ = 250. *B*: neuron generated from the average conductances of all the one-spike bursters ($g_{max}Na$ = 283, $g_{max}Kd$ = 38.0, $g_{max}Ca$ = 3.45, $g_{max}A$ = 26.2, $g_{max}KCa$ = 146). The *insets* are 50 ms in width and have tick marks at −30 mV. *Right panels*: histograms showing the values of the Na$^+$ and 4 times the delayed-rectifier K$^+$ maximal conductances.
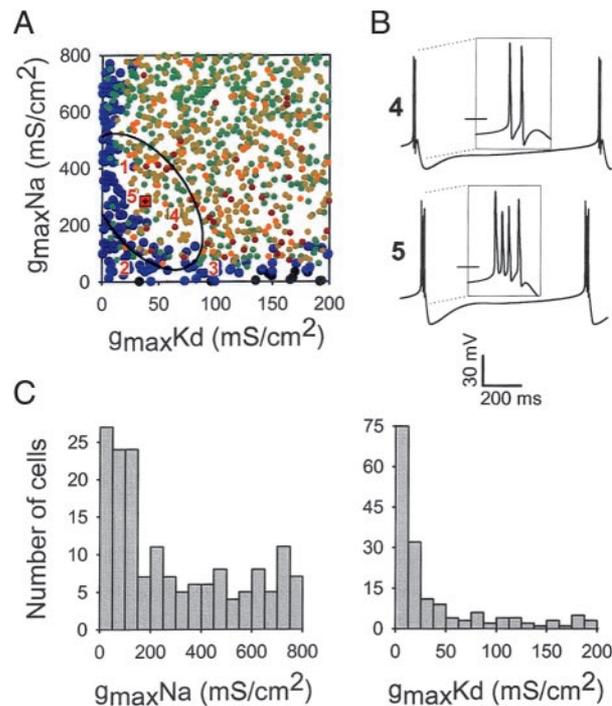

FIG. 3. Single and multiple spike bursters. *A*: number of spikes per burst (0, black; 1, blue; 2, green; 3, olive; 4, orange; 5, burgundy) for bursting neurons with the indicated values of $g_{max}Na$ and $g_{max}Kd$. The difference in dot sizes is for ease of visualization only. One-spike bursters (blue) lie in an L-shaped region that does not include its mean (red square with cross, which generates the activity seen in Fig. 2*B*) or most of its 1 SD covariance ellipse (black oval curve; individual conductance SDs in mS/cm^2 are σ_{Na} = 241; σ_{Kd} = 50.6; σ_{Ca} = 1.18; σ_A = 20.1; σ_{KCa} = 88.6). Bursters with more than 1 spike per burst appear randomly distributed in this 2-dimensional projection. Labeled cells (red numbers 1–5) correspond to voltage traces in Fig. 2*A* and Fig. 3*B*. *B*: voltage traces for 2 neurons (a two-spike burster and a four-spike burster) with conductances lying within 1 SD of the mean (conductance values in mS/cm^2: 4, $g_{max}Na$ = 229, $g_{max}Kd$ = 60.2, $g_{max}Ca$ = 2.72, $g_{max}A$ = 36.0, $g_{max}KCa$ = 158; 5, $g_{max}Na$ = 296, $g_{max}Kd$ = 26.4, $g_{max}Ca$ = 2.89, $g_{max}A$ = 15.5, $g_{max}KCa$ = 90.6). The *insets* are 50 ms in width and have tick marks at −30 mV. *C*: distribution histograms showing the number of one spike bursting neurons with the indicated amount of $g_{max}Na$ (*left*) or $g_{max}Kd$ (*right*).

with a certain number of spikes per burst. From these runs, we found that 164 model neurons fire one spike per burst, and we used these as our set of "identified one-spike bursting neurons" (Fig. 2*A, traces 1–3* represent 3 examples). The one-spike bursters display similar firing patterns (Fig. 2*A, left*) despite having very different maximal conductances (Fig. 2*A, right*).

We used the conductance data from these one-spike bursters to represent recordings from the same identified neuron in different preparations. Conventionally, these data would be used to construct a single model neuron with maximal conductances equal to the averages of the measured values. Following this procedure, we built a model neuron using the average maximal conductances of our 164 model neuron set. Surprisingly, this average model is not itself a one-spike burster, but instead is a three-spike burster (Fig. 2*B*). Moreover, we found that only 28% of 500 additional model neurons constructed from randomly sampled points within the 1 SD ellipse defined by the covariances of the sampled one-spike bursters were themselves one-spike bursters (a 2-dimensional projection of this ellipse is shown in Fig. 3*A*).

Figure 3 illustrates why averaging fails in this case. Figure 3*A* shows the Na$^+$ maximal conductance, $g_{max}Na$, and the

delayed rectifier K$^+$ maximal conductance, $g_{max}Kd$, of all of the bursting neurons from the 2,000 runs of the model. The one-spike bursters (Fig. 2*A*) are shown in blue, while multiple-spike bursters (Fig. 3*B*) are colored according to their number of spikes. The one-spike bursters are defined almost exclusively by low values of $g_{max}Na$ and/or $g_{max}Kd$ (Figs. 2*A* and 3*A*). As a result, their maximal conductances lie in an L-shaped (concave) region. Consequently, in this data set, the mean (red square with cross in Fig. 3*A*) and most of the points within 1 SD of the mean (black ellipse in Fig. 3*A*) fall outside the concave region defining the one-spike bursters. Figure 3*C* shows distributions for $g_{max}Na$ and $g_{max}Kd$ alone and demonstrates that the 164 one-spike bursters do not fall into 2 separate classes on the basis of single-conductance measurements.

DISCUSSION

The essential feature that leads to the failure of averaging in this study is the concave, L-shaped region of parameter space occupied by the one-spike bursters. This shape defines a non-linear relationship between the values of $g_{max}Na$ and $g_{max}Kd$ that is not captured by standard statistical measures such as means and variances (Fig. 3*A*). The averaged model (Fig. 2*B*) fails because the process of averaging does not account for this nonlinear relationship (Beer et al. 1999; Foster et al. 1993; Goldman et al. 2001). Variances fail to describe the relationship between $g_{max}Na$ and $g_{max}Kd$ because they only characterize variability of linear combinations of parameters that are assumed to be independent. Multimodal distributions of individual variables might serve as an indication that averaging may fail. However, unimodal distributions, such as those in Fig. 3*C* or even normal distributions, can lead to a failure of averaging, due to correlations not revealed by the individual distributions. This happens, for example, if the values near the mean of one variable are correlated with values within the tails of the distribution for a second variable.

Capturing the nonlinear relationships between system components may be essential for understanding system function in many biological systems. In the case of our model, individual measurements of $g_{max}Na$ in one group of cells and of $g_{max}Kd$ in another group only reveal a tendency for each conductance to have low values (Fig. 3*C*). Simultaneous measurements of these conductances in each cell studied (Fig. 3*A*) reveal that $g_{max}Na$ and $g_{max}Kd$ act together as a switch between single- and multi-spike bursting, with multi-spike bursting arising only when $g_{max}Na$ and $g_{max}Kd$ are both sufficiently large (enough fast inward Na$^+$ current to produce a 2nd action potential within the burst and enough fast outward K$^+$ current to repolarize the cell, allowing the 2nd action potential to be produced).

The issues raised by this paper are not specific to biophysical measurements of conductances in neurons or to the construction of neuronal models; they may be relevant to understanding many complex biological systems (Koch and Laurent 1999; Weng et al. 1999). We do not know how frequently averaging

will fail in complex systems, but it may occur more often than is typically suspected (Beer et al. 1999; Chiel et al. 1999; Foster et al. 1993). Perhaps some of the fine tuning required to make models reproduce experimentally observed activity may be correcting for failures of averaging rather than measurement errors. Of course, using averaged parameters in models often works well. In our example, averaging fails for one-spike bursters but works for multiple-spike bursters in the sense that a model built by averaging parameters over all *n*-spike bursters (for $n > 1$) produces *n* spikes per burst.

Averaging will fail whenever the mean of the distribution of relevant data points lies outside the region they occupy. Standard statistical measures do not indicate when this occurs because they do a poor job of characterizing the boundary of a region. However, scatter plots of the relevant parameters, as used here, should be sufficient to reveal a failure of averaging by showing regional boundaries. To characterize a system when averaging fails, it is critical to measure multiple system components together in the same preparation, even though this may be technically challenging. When simultaneous measurements are not available, modeling studies can help uncover the relationships between model parameters that must be characterized to account for observed system behavior.

REFERENCES

BEER RD, CHIEL HJ, AND GALLAGHER JC. Evolution and analysis of model CPGs for walking. II. General principles and individual variability. *J Comput Neurosci* 7: 119–147, 1999.
BHALLA US AND BOWER JM. Exploring parameter space in detailed single neuron models: simulations of the mitral and granule cells of the olfactory bulb. *J Neurophysiol* 69: 1948–1965, 1993.
CHIEL HJ, BEER RD, AND GALLAGHER JC. Evolution and analysis of model CPGs for walking. I. Dynamical modules. *J Comput Neurosci* 7: 99–118, 1999.
FOSTER WR, UNGAR LH, AND SCHWABER JS. Significance of conductances in Hodgkin-Huxley models. *J Neurophysiol* 70: 2502–2518, 1993.
GARDNER D. *The Neurobiology of Neural Networks.* Cambridge, MA: MIT Press, 1993, p. 21–70.
GOLDMAN MS, GOLOWASCH J, MARDER E, AND ABBOTT LF. Global structure, robustness, and modulation of neuronal models. *J Neurosci* 21: 5229–5238, 2001.
GOLOWASCH J, ABBOTT LF, AND MARDER E. Activity-dependent regulation of ionic currents in an identified neuron of the stomatogastric ganglion of the crab *Cancer borealis*. *J Neurosci* 19 (RC33): 31–35, 1999.
KOCH C AND LAURENT G. Complexity and the nervous system. *Science* 284: 96–98, 1999.
LIU Z, GOLOWASCH J, MARDER E, AND ABBOTT LF. A model neuron with activity-dependent conductances regulated by multiple calcium sensors. *J Neurosci* 18: 2309–2320, 1998.
TURRIGIANO GG, LEMASSON G, AND MARDER E. Selective regulation of current densities underlies spontaneous changes in the activity of cultured neurons. *J Neurosci* 15: 3640–3652, 1995.
WENG G, BHALLA US, AND IYENGAR R. Complexity in biological signaling systems. *Science* 284: 92–96, 1999.